

# Development of a process map: a step towards a regime map for steady-state high shear wet twin screw granulation

Ashish Kumar<sup>a,b</sup>, Jens Dhondt<sup>b,1</sup>, Jurgen Vercruyse<sup>c</sup>, Fien De Leersnyder<sup>b</sup>, Valérie Vanhoorne<sup>c</sup>, Chris Vervaet<sup>c</sup>, Jean Paul Remon<sup>c</sup>, Krist V. Gernaey<sup>d</sup>, Thomas De Beer<sup>b,1</sup>, Ingmar Nopens<sup>a,\*</sup>

<sup>a</sup>*BIOMATH, Department of Mathematical Modelling, Statistics and Bioinformatics, Faculty of Bioscience Engineering, Ghent University, Coupure Links 653, B- 9000 Gent, Belgium*

<sup>b</sup>*Laboratory of Pharmaceutical Process Analytical Technology, Department of Pharmaceutical Analysis, Faculty of Pharmaceutical Sciences, Ghent University, Ottergemsesteenweg 460, B-9000 Ghent, Belgium*

<sup>c</sup>*Laboratory of Pharmaceutical Technology, Department of Pharmaceutics, Faculty of Pharmaceutical Sciences, Ghent University, Ottergemsesteenweg 460, B-9000 Ghent, Belgium*

<sup>d</sup>*CAPEC-PROCESS Research Center, Department of Chemical and Biochemical Engineering, Technical University of Denmark, DK-2800 Kongens Lyngby, Denmark*

---

## Abstract

Twin-screw granulation is an emerging continuous granulation technique in the pharmaceutical industry. The flexibility in process settings such as the binder addition method (wet vs. dry), screw configuration, screw speed and material throughput allows to modify the granule size and shape. However, twin-screw granulation, being a rather new granulation technique, is not yet as well understood as batch-wise high shear wet granulation. Furthermore, most of the studies performed on twin-screw granulation are limited to a certain design and scale of the twin-screw granulator. In this study, in order to improve the understanding about the granulation process and to comprehend the applicability and limits of

---

\*Email address: [ingmar.nopens@ugent.be](mailto:ingmar.nopens@ugent.be), Tel.: +32 (0)9 264 61 96; fax: +32 (0)9 264 62 20

Email addresses: [ashish.kumar@ugent.be](mailto:ashish.kumar@ugent.be) (Ashish Kumar), [jensj.dhondt@ugent.be](mailto:jensj.dhondt@ugent.be) (Jens Dhondt), [jurgen.vercruyse@ugent.be](mailto:jurgen.vercruyse@ugent.be) (Jurgen Vercruyse), [fien.deleersnyder@ugent.be](mailto:fien.deleersnyder@ugent.be) (Fien De Leersnyder), [valerie.vanhoorne@ugent.be](mailto:valerie.vanhoorne@ugent.be) (Valérie Vanhoorne), [chris.vervaet@ugent.be](mailto:chris.vervaet@ugent.be) (Chris Vervaet), [jeanpaul.remon@UGent.be](mailto:jeanpaul.remon@UGent.be) (Jean Paul Remon), [kvg@kt.dtu.dk](mailto:kvg@kt.dtu.dk) (Krist V. Gernaey), [thomas.debeer@ugent.be](mailto:thomas.debeer@ugent.be) (Thomas De Beer)

URL: [www.biomath.ugent.be](http://www.biomath.ugent.be) (Ingmar Nopens)

<sup>1</sup>Shared first and last authorships

the process variables in a scale independent manner, the regime theory was applied to one specific twin-screw granulator equipment. In this study,  $\alpha$ -lactose monohydrate was granulated with polyvinylpyrrolidone (2.5%, w/w) as binder. The screw configuration of the 25 mm diameter co-rotating twin-screw granulator from the ConsiGma<sup>TM</sup>-25 unit consisted of one or two kneading zones of six kneading elements each (1×6 and 2×6, respectively), at a stagger angle of 60 degrees. The specific mechanical energy, which involves the combination of screw speed, material throughput and torque required to rotate the screws was correlated with the applied liquid-to-solid ratio to present process maps. The study suggested that, despite an increase in the granule size by the increasing liquid-to-solid ratio, most of the liquid contributes to formation of oversized granules. Therefore, keeping the liquid-to-solid ratio in a lower range and increasing the energy input to the system can be effectively used to lower the mean granule size. Changes in the screw geometry should also be explored to improve solid liquid mixing and breakage of oversized granules to narrow the width of the size distribution. Since, such a process map is limited to a selected formulation and equipment design, process maps based on several formulations and mechanistic mathematical modelling tools should be applied to identify the mechanisms and relevant dimensionless groups that control granule attributes, with the ultimate aim of producing a generalised regime map.

*Keywords:* continuous wet granulation, specific mechanical energy, liquid-to-solid ratio, granule size distribution

---

<sup>1</sup> **1. Introduction**

<sup>2</sup> Within the pharmaceutical industry, granulation is a key step for the production of solid  
<sup>3</sup> dosage forms [1]. However, the granulation process is rather complex making the prediction  
<sup>4</sup> of the granule quality attributes (e.g. granule size distribution (GSD), density, flow, etc.)  
<sup>5</sup> based on the applied process settings challenging. Therefore, process development for a new  
<sup>6</sup> formulation and equipment is mainly performed using the trial and error approach to find  
<sup>7</sup> the optimal conditions providing granules with a desired set of properties. Subsequently,  
<sup>8</sup> during scaling-up to commercial scale equipment, time consuming studies are needed to  
<sup>9</sup> obtain comparable granule quality at the larger scale equipment [1]. Although continuous  
<sup>10</sup> processing is still in its infancy in the pharmaceutical industry, it holds a great potential  
<sup>11</sup> due to various quality and economics related benefits. Compared to conventionally used  
<sup>12</sup> batch techniques, continuous processes can eliminate scale-up issues and storage of inter-  
<sup>13</sup> mediates [2, 3], while steady-state operation results in more uniform granule properties [4].  
<sup>14</sup> Hence, continuous twin-screw granulation has received increased attention as it can be di-  
<sup>15</sup> rectly coupled to a dryer, milling unit and tabletting machine, thus creating a continuous  
<sup>16</sup> 'from-powder-to-tablet' manufacturing line. Also, the two screws in a twin-screw granulator  
<sup>17</sup> (TSG) are self-cleaning, and therefore minimising accumulation of material and potential  
<sup>18</sup> issues with material degradation [5].

<sup>19</sup>  
<sup>20</sup> Unlike batch-wise equipment, granulation in a TSG is not yet very well understood. Several  
<sup>21</sup> researchers have investigated various aspects of TSG including the effect of key formulation  
<sup>22</sup> variables [6–9], screw configurations [5, 10–13] and process settings [4, 14]. However, all these  
<sup>23</sup> studies have been performed using granulators with different dimensions leading to differ-  
<sup>24</sup> ences in the scale and limits of variations in the parameters across studies. Thus, in order  
<sup>25</sup> to comprehend the applicability and limits of variables over different scales and to improve  
<sup>26</sup> the understanding regarding the granulation process in terms of development of generally  
<sup>27</sup> applicable knowledge, the regime theory is applied. A regime theory is presented as a map  
<sup>28</sup> which semi-quantitatively explains the variation in granulation behaviour during operation

<sup>1</sup> [15]. By developing a regime map, it becomes possible to correlate the input variables of the  
<sup>2</sup> process and equipment with the granule characteristics [15]. The mechanistic basis derived  
<sup>3</sup> from a regime map is better than data-driven models, and the granulation design space  
<sup>4</sup> can be determined more effectively with fewer experiments [16]. Initially, regime maps were  
<sup>5</sup> introduced for nucleation and granule growth behaviour [1, 17–19]. Although these regime  
<sup>6</sup> maps do not cover equipment design and require an experimental validation with a range  
<sup>7</sup> of materials and different granulation conditions to locate the change in regime boundaries  
<sup>8</sup> when subjected to these variations, they have been successful in qualitatively describing  
<sup>9</sup> granulation under a given set of conditions. Later, an equipment specific granulation regime  
<sup>10</sup> map resolving general effects of parameters such as impeller speed and liquid-to-solid ratio  
<sup>11</sup> (L/S) ratio in a high shear granulator was proposed by Tu et al. [20].

<sup>12</sup>  
<sup>13</sup> To extend this approach of knowledge development to the twin-screw granulation process,  
<sup>14</sup> Dhenge et al. [6, 7] developed two regime maps for the TSG, first with a twin-screw contain-  
<sup>15</sup> ing conveying elements only and the other in which both conveying and mixing elements were  
<sup>16</sup> present. Both these regime maps mapped the granulation characteristics as under-wetted,  
<sup>17</sup> nuclei, crumb, granules and over-wetted or paste based on the relation between the modified  
<sup>18</sup> deformation value and the pore saturation. The modified deformation value was calculated  
<sup>19</sup> as  $\beta = \frac{T}{V} \times \frac{1}{\tau}$ , where  $T$ ,  $V$ ,  $\tau$  are torque (Nm), volume of material in the barrel ( $m^3$ ) and  
<sup>20</sup> the strength of the granules (MPa), respectively. The pore saturation was assumed to be  
<sup>21</sup> a function of L/S and viscosity of the granulation liquid, i.e.  $L/S \times$  viscosity. Dhenge et  
<sup>22</sup> al. [7] observed that without mixing zone the wet, big, loose and weak agglomerates termed  
<sup>23</sup> as nuclei were produced in different amounts based on the deformation values ( $\beta$ ). It was  
<sup>24</sup> suggested in the other regime map by Dhenge et al. [6] that a transition of regimes can be  
<sup>25</sup> achieved by applying changes in the screw configuration and the process conditions (Fig. 1).

<sup>26</sup> [Figure 1 about here.]

<sup>27</sup> Tu et al. [21], following the earlier approach of building a regime map for a high shear gran-  
<sup>28</sup> ulator [20], also proposed a regime map for a co-rotating TSG. The studied parameters were

1 L/S ratio, screw speed and screw configuration. Hereby, a reduction in screw speed led to  
2 an increased fill level of the TSG barrel which showed a direct correlation with an increase  
3 of frictional force and torque. Similarly, an increase in the L/S ratio correlated with a high  
4 fill level and torque. Depending on the screw configuration three regimes were suggested:  
5 granulation, extrudate and blocked regime. Granules with a large size and narrow GSD  
6 were obtained for increased binder addition and screw speed and using a screw configura-  
7 tion that provided sufficient mixing [21]. However, unlike dimensionless numbers used in all  
8 the previous work on development and parameters with intensive properties used by Dhenge  
9 et al. [6, 7], the regime map by Tu et al. [21] used scale-dependent parameters, such as screw  
10 speed and torque, for the development of this regime map. This further extends the current  
11 limitation of regime maps from uncomprehended regime boundaries for a range of materials  
12 to their inapplicability in explaining a TSG process with a different screw diameter, which  
13 does not operate under similar operational conditions. Also, a bi-modal GSD was obtained  
14 for several runs reported in this study. Thus, using only the mean granule size is not valid for  
15 granule size characterisation in many of the reported experimental conditions. The regime  
16 maps proposed by Dhenge et al. [6, 7] and Tu et al. [21] also indicated that a significant effort  
17 is still needed to identify the controlling parameters of twin-screw granulation for different  
18 combinations of process and equipment settings in order to propose a granulation regime  
19 map.

20

21 In the current study, the effect of four input variables (screw configuration ( $1 \times 6$  and  $2 \times 6$   
22 kneading discs), liquid-to-solid ratio (8-10 %), powder feed rate (10-25 kg/h), and screw  
23 speed (500-900 rpm)) on the GSD was evaluated. Afterwards, GSD results were used for  
24 mapping of granulation regimes when changes in process parameters were applied. Scale-  
25 independent parameters (specific mechanical energy (SME) and L/S) were chosen to expand  
26 the applicability to multiple TSG scales. As the present study provides a guidance towards  
27 mapping the wet granulation process in a TSG with one formulation and the results should  
28 be examined with a range of materials, the presented maps are identified as "process maps".  
29 Finally, the relevance of such process maps and the required efforts for developing a regime

<sup>1</sup> map are identified and discussed.

<sup>2</sup> **2. Materials and methods**

<sup>3</sup> *2.1. Pharmaceutical model formulation*

<sup>4</sup>  $\alpha$ -lactose monohydrate (Pharmatose 200M, DFE-Pharma, Caldic, Hemiksem, Belgium)  
<sup>5</sup> was used as a model excipient and polyvinylpyrrolidone (PVP) (Kollidon<sup>TM</sup>30, BASF, Lud-  
<sup>6</sup> wigshafen, Germany) was used as a binder (1.5 %, w/w). An aqueous PVP solution with a  
<sup>7</sup> concentration of 15.8, 14.3 and 13.0 % (viscosity 10.3, 8.3 and 6.9 mPa.s respectively at 25  
<sup>8</sup> °C, as per MSDS) was used as granulation liquid to achieve 8, 9 and 10 % L/S ratio. The  
<sup>9</sup> PVP solutions were prepared using a rotor-stator mixer (Silverson L4R, USA).

<sup>10</sup> *2.2. Continuous twin-screw granulation*

<sup>11</sup> Granulation experiments were performed using a 25 mm diameter co-rotating TSG, which  
<sup>12</sup> is the granulation module of the ConsiGma<sup>TM</sup>-25 unit (GEA Pharma Systems, Collette<sup>TM</sup>,  
<sup>13</sup> Wommelgem, Belgium). The granulator screws have a length-to-diameter ratio of 20:1. The  
<sup>14</sup> TSG barrel consists of a feed segment, where the powder enters the barrel and is transported  
<sup>15</sup> to the work segment. For the screw configuration with 6 kneading elements one kneading  
<sup>16</sup> block was used, and for 12 kneading elements two kneading blocks each consisting of 6  
<sup>17</sup> kneading elements were used in the work segment. Both kneading zones were separated  
<sup>18</sup> by a conveying element block (Length = 1.5D) to limit the accumulation of the material.  
<sup>19</sup> The stagger angle of the kneading elements was fixed at 60°. After the kneading zone(s) a  
<sup>20</sup> conveying element was implemented together with 2 narrow kneading discs (Length = D/6  
<sup>21</sup> for each kneading disc) in the end of the screw in order to reduce the amount of oversized  
<sup>22</sup> agglomerates, as reported by Van Melkebeke et al. [2]. Here, the granulation liquid is  
<sup>23</sup> added to the powder and is further intensively mixed by a combination of kneading discs  
<sup>24</sup> and transport screws. The barrel jacket was preheated to 25 °C. During processing, pure  $\alpha$ -  
<sup>25</sup> lactose monohydrate was gravimetrically fed into the granulator by using a twin-screw feeder  
<sup>26</sup> (KT20, K-Tron Soder, Niederlenz, Switzerland). Distilled water with PVP as granulation  
<sup>27</sup> liquid was pumped into the screw chamber by using a peristaltic pump (Watson Marlow,

<sup>1</sup> Cornwall, UK) and silicon tubings connected to 1.6 mm nozzles. The granulation liquid was  
<sup>2</sup> added (8-10 % w/w) before the first kneading block (Fig. 2) by dripping through two liquid  
<sup>3</sup> feed ports, each port located centrally on top of each screw in the barrel. The torque on the  
<sup>4</sup> granulator screws is primarily related to the number of kneading discs and filled channel of  
<sup>5</sup> the conveying elements upstream. The TSG has a built-in torque gauge (accuracy  $\pm 0.25$   
<sup>6</sup> %FS ( $\pm 0.5$  %FS for 2 Nm and below), TorqSense RWT310/320, UK) and the steady state  
<sup>7</sup> criteria were decided based on the equilibration of the measured torque on the granulator  
<sup>8</sup> screws. The torque values obtained after equilibration of the process were averaged to give  
<sup>9</sup> the working torque during each run (see supplementary Table S1).

<sup>10</sup> [Figure 2 about here.]

### <sup>11</sup> 2.3. Experimental design

<sup>12</sup> The experimental range for the performed screening design was determined by carrying  
<sup>13</sup> out preliminary tests. The studied process variables include powder feed rate (10, 17.5, 25  
<sup>14</sup> kg/h), liquid addition (8, 9 and 10 %), screw configuration (1 $\times$ 6 and 2 $\times$ 6 kneading discs) and  
<sup>15</sup> screw speed (500, 700 and 900 rpm). Granules were collected at the outlet of the TSG and  
<sup>16</sup> oven dried for 24 h at 40 °C. A full-factorial experimental design, with 54 experiments, was  
<sup>17</sup> used to evaluate the influence of the different process variables upon the granulation process  
<sup>18</sup> and the GSD. The experimental data were fitted using the most appropriate multiple linear  
<sup>19</sup> regression (MLR) model (using Modde 9.0 software by Umetrics, Umeå, Sweden) [22]. 4D  
<sup>20</sup> Contour plots were made to display the responses for the four varying factors simultaneously.

### <sup>21</sup> 2.4. Determination of torque and specific mechanical energy

<sup>22</sup> To evaluate the granulation process, the torque on the screws at the work segment was  
<sup>23</sup> recorded (1s interval). After steady-state was reached, the torque values were averaged.  
<sup>24</sup> These represent the energy required to rotate the screws in the barrel, and represent the  
<sup>25</sup> frictional forces on the material during processing. The SME, which is a scale-independent  
<sup>26</sup> measure of energy introduced to the system during the granulation process [23], was calcu-

1 lated as follows

$$\text{SME (kJ/kg)} = \text{motor power rating} \times \% \text{ torque} \times \frac{\text{RPM}_{\text{oper}}}{\text{RPM}_{\text{max}}} \times \frac{\text{gearbox efficiency}}{\text{material throughput}} \quad (1)$$

2 where the TSG had a motor rating (MR) of 2.2 kW and a maximum screw speed,  $\text{RPM}_{\text{max}}$   
3 of 1000 RPM. The operational screw speed,  $\text{RPM}_{\text{oper}}$  and material throughput (kg/h) varied  
4 based on the processing setting. The gearbox of a TSG transmits energy from the motor  
5 to the screws, and is hence critical for achieving the desired screw speed and energy input.  
6 Based on the technical specification of the granulator drive (POSITWIN, Brevini Power  
7 Transmission), the gearbox efficiency is set at 0.98 [24].

8 *2.5. Particle size analysis*

9 For each experiment, the GSD was determined using the sieve analysis method (Retsch  
10 VE 1000 sieve shaker, Haan, Germany). Granule samples (100 g) were placed on a shaker  
11 for 5 min at an amplitude of 2 mm using a series of sieves (150, 250, 500, 710, 1000, 1400  
12 and 2000  $\mu\text{m}$ ). The amount of granules retained on each sieve was determined. All granule  
13 batches were measured in triplicate. The fractions <150, 150-1400 and >1400  $\mu\text{m}$  were  
14 defined as the amount of fines, useful fraction for tableting or yield fraction and oversized  
15 fraction, respectively. Also, three quartile values ( $D_{25}$ ,  $D_{50}$  and  $D_{75}$ ), corresponding to the  
16 25, 50 and 75 percentiles respectively of the obtained GSD were calculated to build the  
17 regime map. The width of the GSD was measured as percentile ratio, a relative measure of  
18 the distribution width ( $D_{75}/D_{25}$ ) [25]. The percentile ratio value approaches unity as the  
19 distribution becomes narrower.

20 *2.6. Spatial interpolation and verification*

21 The 'natural neighbour interpolation' method based on Delaunay triangulation was used  
22 for the spatial interpolation in the granulation regime map [26]. This has advantages over  
23 simpler methods of interpolation (such as nearest-neighbour interpolation), as it provides a

<sup>1</sup> smoother approximation to the underlying function. The basic equation in 2D is given as:

$$G(x, y) = \sum_{i=1}^n w_i f(x_i, y_i) \quad (2)$$

<sup>2</sup> where  $G(x, y)$  is the estimate for the (L/S, SME) ranges,  $w_i$  are the weights and  $f(x_i, y_i)$  are  
<sup>3</sup> the known granule size values at  $L/S_i$ ,  $SME_i$ . The weights,  $w_i$ , were calculated by finding how  
<sup>4</sup> much of each of the surrounding areas is taken when inserting  $(x, y)$  into the tessellation. To  
<sup>5</sup> assess the accuracy of the interpolation, 14 measured points were removed from the known  
<sup>6</sup> input (total 54 points), and the regime map was re-created using the remaining points.  
<sup>7</sup> The root mean square error (RMSE) of the predicted values in the regime map with the  
<sup>8</sup> removed measured points and the actual values was calculated and normalised to quantify  
<sup>9</sup> the accuracy.

### <sup>10</sup> 3. Results and discussion

#### <sup>11</sup> 3.1. Effect on torque

<sup>12</sup> The highest torque values were obtained at maximum fill ratio of the barrel i.e., low screw  
<sup>13</sup> speed and high throughput together with the highest restriction to the material flow by using  
<sup>14</sup> the 2×6 configuration (Fig. 3). Low screw speed led to low conveying rate, whereas high  
<sup>15</sup> material throughput resulted in high load on the screws. Furthermore, increasing L/S ratio  
<sup>16</sup> caused sluggish flow of the material and using a second kneading block on the granulator  
<sup>17</sup> screws resulted in a high restriction to the material flow [27, 28]. The change in torque level  
<sup>18</sup> by different factors was more explicit at low screw speed. On the other hand, the torque  
<sup>19</sup> level dropped when the screw speed was increased or when either throughput or L/S was  
<sup>20</sup> reduced.

<sup>21</sup> [Figure 3 about here.]

#### <sup>22</sup> 3.2. Effect on granule size distribution

<sup>23</sup> An increase in L/S ratio caused reduction in fines and an increase in the oversized fraction  
<sup>24</sup> (Fig. 4). The effect of changing L/S ratio on GSD was most evident for the runs performed

1 at low screw speed (500 RPM) and higher throughputs (17.5 and 25 kg/h). However, the  
2 yield fraction was least affected by the additional granulation liquid (i.e., at high L/S).  
3 Hence, other process parameters play a critical role in increasing the yield fraction. These  
4 process parameters are mainly responsible for a change in the fill level and distributive as  
5 well as dispersive mixing of material inside the TSG barrel. Thus, a brief analysis of the  
6 effect of various process parameters under study on each size fraction is presented below.

7 [Figure 4 about here.]

8 *3.2.1. Effect on fines*

9 A higher amount of fines was produced by using the screw configuration with  $1 \times 6$  knead-  
10 ing discs at a low L/S and screw speed ( $N_{RPM}$ ) (Fig. 5). However, at increased L/S as well  
11 as at increased throughput a reduction in the amount of fines was obtained. For the screw  
12 configuration with  $2 \times 6$  kneading discs, the amount of fines mostly remained at a low level  
13 due to better mixing of powder and granulation liquid. An increase in screw speed from 500  
14 to 900 rpm caused an increase in fines at low L/S ratio due to attrition of bigger granules  
15 caused by the higher impact of the screws at high screw speed. This can also occur due  
16 to an increased weakness of the granules having insufficient moisture content [29]. Further-  
17 more, if fines are created at low L/S they will not stick to other granules because of lack  
18 of granulation liquid at the surface of these granules. In contrast, fines that are created at  
19 high L/S ratio can still be captured again because of the presence of granulation liquid at  
20 the surface.

21 [Figure 5 about here.]

22 *3.2.2. Effect on yield fraction*

23 The yield fraction of the granules remained low despite higher mechanical shear caused by  
24 the additional kneading block present in the screw configuration with  $2 \times 6$  kneading discs.  
25 However, an increase in the yield fraction was observed when increasing screw speed for  
26 both screw configurations suggesting that along with good mixing, shear breaking of bigger  
27 lumps is a prominent mechanism leading to a higher yield fraction. Beside a lower amount

1 of fines, an increase in L/S also reduced the yield fraction. This indicates that additional  
2 granulation liquid directly contributed to formation of oversized granules. Therefore, it  
3 was concluded that the basic granulation mechanism of growth by nucleation followed by  
4 aggregation as observed in high-shear mixers is not the primary mechanism of the twin-  
5 screw granulation to control the yield. Breakage of oversized lumps is required to achieve  
6 a high yield inside a TSG. Additionally, when the screw speed was low, an increase in L/S  
7 ratio showed only a minor influence on the yield fraction (causing less mixing between the  
8 powder and the granulation liquid) for both screw configurations despite a change in the  
9 material throughput. An increase in the throughput caused a reduction in yield fraction for  
10 a low number ( $1 \times 6$ ) of kneading discs whereas an increase in yield fraction was observed  
11 for a high number ( $2 \times 6$ ) of kneading discs. This was again due to inferior mixing due to a  
12 smaller mixing zone in the TSG. An increase in screw speed lowered the fill ratio due to the  
13 higher conveying rate, and thus increased the mixing efficiency and resulting yield fraction  
14 of granules.

15 [Figure 6 about here.]

16 *3.2.3. Effect on oversized fraction*

17 Although twin-screw granulation always resulted in a large fraction of oversized granules  
18 ( 30-60% of the produced granules), increasing the L/S ratio, i.e., adding more granulation  
19 liquid, contributed most to the formation of the oversized granule fraction (Fig. 7). When a  
20 restriction to the material flow was introduced by the additional kneading block in the screw  
21 configuration with  $2 \times 6$  kneading discs combined with a high amount of granulation liquid,  
22 more oversized granules were obtained. This suggests that the distributive characteristics  
23 of the kneading elements were insufficient to efficiently break the larger wetted lumps which  
24 resulted in more oversized granules. However, an increase in the screw speed decreased the  
25 amount of oversized granules produced to a certain extent. This was due to a reduction in  
26 the fill ratio and an improved shear mixing of the granulation mixture and the liquid. For  
27 the same reason, an increase in throughput causing a high fill ratio yielded an increased  
28 oversized fraction in the produced granules.

<sup>1</sup> [Figure 7 about here.]

<sup>2</sup> *3.3. Effect on specific mechanical energy level*

<sup>3</sup> The SME is a direct measure of the amount of power being introduced by the motor  
<sup>4</sup> into each kilogram of material being processed inside the TSG. A gradual increase in screw  
<sup>5</sup> speed led to a gradual increase in the SME level (Fig. 8). However, for fixed process settings  
<sup>6</sup> (screw speed and throughput), the change in screw configuration caused major changes in  
<sup>7</sup> the SME levels such that their range for the screw with  $2 \times 6$  kneading discs was much higher  
<sup>8</sup> than for the  $1 \times 6$  kneading discs screw configuration. Beside screw configuration and speed,  
<sup>9</sup> other process parameters such as material throughput and L/S ratio also affected the SME  
<sup>10</sup> level. The material throughput and L/S ratio contribute to the restriction to the material  
<sup>11</sup> flow inside the granulator, hence changing the load on the screws and energy input to the  
<sup>12</sup> material. Due to these encompassing characteristics of the SME, it was used along with the  
<sup>13</sup> L/S ratio to characterize the granulation process in the TSG in the next section.

<sup>14</sup> [Figure 8 about here.]

<sup>15</sup> *3.4. Process mapping based on GSD, L/S and SME*

<sup>16</sup> The granulation process maps for the D<sub>25</sub>, D<sub>50</sub> and D<sub>75</sub> for the  $1 \times 6$  and  $2 \times 6$  screw  
<sup>17</sup> configurations are shown in Fig. 9. The effect of changes in L/S ratio and SME inputs on  
<sup>18</sup> GSD is given in these maps. The accuracy of the interpolated map was tested and the  
<sup>19</sup> RMSE for the D<sub>25</sub>, D<sub>50</sub> and D<sub>75</sub> process map of the  $1 \times 6$  screw configuration was found to  
<sup>20</sup> be 3.36, 1.83 and 0.48  $\mu\text{m}$ , respectively. The RMSE for the D<sub>25</sub>, D<sub>50</sub> and D<sub>75</sub> process map  
<sup>21</sup> of the  $2 \times 6$  screw configuration was found to be 3.05, 1.30 and 0.07  $\mu\text{m}$ , respectively.  
<sup>22</sup> For all the SME and L/S levels, the D<sub>25</sub> values ranged from 300 to 600  $\mu\text{m}$  in case of  
<sup>23</sup> the  $1 \times 6$  screw configuration. However, when an additional kneading block was used ( $2 \times 6$   
<sup>24</sup> kneading discs) leading to better mixing, a high SME input and L/S ratio caused a further  
<sup>25</sup> increase in the D<sub>25</sub> value (up to 900  $\mu\text{m}$ ). This indicates that besides increased liquid and  
<sup>26</sup> energy input, the screw configuration is also an important factor in reducing the amount  
<sup>27</sup> of fines during granulation. The process maps for D<sub>50</sub> indicate the central tendency of the

<sup>1</sup> GSD change during changes in the process and equipment parameters of the twin-screw  
<sup>2</sup> granulation. These maps suggest that increasing the number of kneading discs at a lower  
<sup>3</sup> L/S range (up to 9%) shifts the median of the GSD profile (i.e.,  $D_{50}$ ) to a larger granule  
<sup>4</sup> size. Moreover, in this range the liquid addition rate is a more dominant factor compared  
<sup>5</sup> to the SME input in deciding the  $D_{50}$  as reflected by minor variation in  $D_{50}$  despite change  
<sup>6</sup> in SME. However, once the L/S is in the intermediate ranges (i.e., 9%) an increase in SME  
<sup>7</sup> resulted in more variation in  $D_{50}$ . This suggests that the more wetted material requires a  
<sup>8</sup> greater amount of energy to distribute the liquid. In lack of additional mixing this liquid  
<sup>9</sup> remains in larger granules, thus having no contribution to size increase. Increase in the  
<sup>10</sup> energy input as achieved by addition of a kneading block squeezed out the interstitial liquid  
<sup>11</sup> to support wet granulation, thus increasing  $D_{50}$ . Such squeezing of the granulation liquid  
<sup>12</sup> towards the granule surface in the kneading zone, which enabled particle layering on the  
<sup>13</sup> freshly wetted granule surface area and hence enlargement, was also observed by El Hagrasy  
<sup>14</sup> et al. [11]. The  $2 \times 6$  screw configuration led to bigger granules and thus higher  $D_{75}$  values  
<sup>15</sup> for all levels of SME and L/S ratio, compared to the  $1 \times 6$  configuration. For the latter,  $D_{75}$   
<sup>16</sup> values corresponded with the oversized fraction ( $> 1400 \mu\text{m}$ ) at medium to high L/S ratio  
<sup>17</sup> and at increased SME input. However, an increase in SME at low L/S caused a reduction  
<sup>18</sup> in  $D_{75}$  values towards the yield fraction size range ( $150-1400 \mu\text{m}$ ). Similar reductions in  
<sup>19</sup>  $D_{75}$  values were observed with increase in SME in case of the  $2 \times 6$  kneading disc screw  
<sup>20</sup> configuration. However, the particle size was still in the oversized granule fraction range.  
<sup>21</sup> At 10 % liquid addition, a minimum of  $520 \mu\text{m}$  in the  $D_{25}$  plot and a maximum of  $2200 \mu\text{m}$   
<sup>22</sup> in the  $D_{75}$  plot was observed. Such a width in granule size indicates that it is better to use  
<sup>23</sup> a lower liquid addition rate. In this regard, 8 to 9 % liquid addition was most optimum,  
<sup>24</sup> with the particle size ranging from 370-1800 and 490-2010  $\mu\text{m}$  respectively. Moreover, the  
<sup>25</sup> geometry of the kneading elements should be modified, both to improve the solid-liquid  
<sup>26</sup> mixing and break the oversized granules more effectively to obtain a higher yield fraction of  
<sup>27</sup> granules.

<sup>28</sup>

[Figure 9 about here.]

1 As indicated in Fig. 9, a higher L/S ratio contributed to the formation of oversized gran-  
2 ules instead of increasing the yield fraction. Therefore, the width of the measured GSD,  
3 which is critical to understand the regime supporting an increase of the yield fraction, was  
4 quantified as percentile ratio ( $D_{75}/D_{25}$ ) (Fig. 10). The percentile ratio map for both screw  
5 configurations (1×6 and 2×6) indicated that the width of the GSD was reduced at higher  
6 L/S. Except for a low L/S ratio and 2×6 screw configuration, the width of the distribution  
7 (i.e., percentile ratio) also reduced with an increase in the SME level, indicating that shear-  
8 driven and energy intensive granulation mechanisms such as attrition and breakage play a  
9 major role during twin-screw granulation [27].

10

11 [Figure 10 about here.]

12 Based on Fig. 9, it is clear that for  $D_{50}$  to correspond to the middle of the fraction of  
13 interest (700 µm) the L/S should be kept at a low level (8 %) whereas the SME level should  
14 range from 30 to 50 kJ/kg. However, this range also gives a much broader GSD (Fig. 10),  
15 which has been discussed in earlier literature [11, 27]. A potential solution to this is to  
16 focus on a change in the kneading elements with the aim of achieving a better mixing of  
17 the solid and the liquid to reduce the amount of fines and to break the oversized granules  
18 as well [5, 12]. According to the correlation of this range of SME with process settings as  
19 shown in Fig. 8, it is suggested that the throughput and screw speed should be increased  
20 simultaneously to increase the amount of granules in the intermediate range, which is the  
21 fraction of interest. By this, a favourable fill level can be achieved and the torque values are  
22 also at an optimum level, thus creating the desired level of energy input to the TSG. The  
23 liquid addition should be kept at an intermediate level as a low liquid addition produces a  
24 low amount of usable granules whereas higher L/S ratio causes higher torque values.

25 **4. Future development: from process map to regime map**

26 The present process map should be regarded as a first step towards a regime map and  
27 should be used with caution. The presented approach in this study can be used as a guid-

1 ance for development of processes applying raw material with properties similar to those  
2 used in this study. The scale-independence of the parameters used in the process map sug-  
3 gests potential application during process scale-up. However, additional experiments on a  
4 large scale granulator should be performed to verify the scale-independency of the devel-  
5 oped process map. Moreover, there is still a need to extend it to better incorporate the  
6 more complex granulation behaviour in TSGs. The formulation properties and operating  
7 variables that control wet granulation behaviour in a TSG are strongly coupled as evidenced  
8 by different results obtained from various studies performed at different process conditions.  
9 Despite the scale-independence of parameters (SME, L/S ratio), more process maps for new  
10 formulations with significantly different raw material properties are necessary due to their  
11 likely differences in the granulation behaviour. This is particularly important as a robust  
12 understanding of the granulation kinetics during solid-liquid mixing in different zones of  
13 the TSG is still lacking. Thus, investigating the effects of liquid and powder characteristics  
14 on other bulk parameters, such as porosity, etc. in the future can ultimately provide a  
15 framework for prediction of overall granule characteristics. While these process maps will  
16 progress our understanding regarding the mechanisms that control granule attributes, for  
17 a reliable and more generalised regime map the most relevant dimensionally homogeneous  
18 terms, i.e. dimensionless groups should be identified (Fig. 11). This is done by preparation  
19 of a "relevance-list" which contains parameters originating from formulation, equipment and  
20 process. For details regarding such an approach the reader is referred to [30].

21

22 [Figure 11 about here.]

23 Additionally, the modular twin-screw design is a feature that is very difficult to incor-  
24 porate in a regime map due to the endless possibilities of variation of the screw design.  
25 However, the geometry strongly affects the flow and mass available for exchange or mixing  
26 between phases, hence the granulation regime. Therefore, the flow regime in the granulator  
27 zones is required to be coupled with the granulation regime for a complete description of the  
28 process. A combination of multi-scale PBM-DEM modelling and the multi-compartment

<sup>1</sup> model incorporating both flow and kinetics is the suggested approach for such applica-  
<sup>2</sup> tions [31–34]. In order to improve the understanding of the twin-screw wet granulation,  
<sup>3</sup> process knowledge should also be further developed both under steady state and dynamic  
<sup>4</sup> conditions. A validated model thus obtained can potentially be used to define the design  
<sup>5</sup> space of the process for the future optimization of the twin-screw granulation process.

<sup>6</sup>

## <sup>7</sup> **5. Conclusions**

<sup>8</sup> In this study, development of a scale-independent wet granulation process map was  
<sup>9</sup> presented. This granulation process map revealed that, although increasing the liquid-  
<sup>10</sup> to-solid ratio strongly drives the granule size distribution of the product towards a large  
<sup>11</sup> mean granule size, by increasing the energy input to the granulator the mean granule size  
<sup>12</sup> can be effectively lowered and also the size distribution can be narrowed. However, since a  
<sup>13</sup> process map is limited to a selected formulation and equipment design, building such process  
<sup>14</sup> maps for a range of formulations and equipment, the most relevant granulation mechanisms  
<sup>15</sup> and dimensionless groups should be identified to propose a generalised regime map in the  
<sup>16</sup> future. With the aim of further process knowledge buildup, the GSD evolution along the  
<sup>17</sup> length of the screws inside the TSG should be experimentally and theoretically mapped in  
<sup>18</sup> order to understand the dominant constitutive mechanisms (such as growth, aggregation  
<sup>19</sup> and breakage) of a twin-screw granulation system.

## <sup>20</sup> **Acknowledgements**

<sup>21</sup> Financial support for this research from the BOF (Bijzonder Onderzoeksfonds Univer-  
<sup>22</sup> siteit Gent, Research Fund Ghent University) is gratefully acknowledged.

<sup>1</sup> **Glossary**

<sup>2</sup>  $N_{RPM}$  screw speed.

<sup>3</sup> **GSD** granule size distribution.

<sup>4</sup> **L/S** liquid-to-solid ratio.

<sup>5</sup> **MLR** multiple linear regression.

<sup>6</sup> **PVP** polyvinylpyrrolidone.

<sup>7</sup> **RMSE** root mean square error.

<sup>8</sup> **SME** specific mechanical energy.

<sup>9</sup> **TSG** twin-screw granulator.

<sup>10</sup> **References**

- <sup>11</sup> [1] S. M. Iveson, J. D. Litster, K. Hapgood, B. J. Ennis, Nucleation, growth and breakage phenomena in  
<sup>12</sup> agitated wet granulation processes: a review, Powder Technol. 117 (1) (2001) 3–39. doi:10.1016/S0032-  
<sup>13</sup> 5910(01)00313-8.
- <sup>14</sup> [2] B. Van Melkebeke, C. Vervaet, J. P. Remon, Validation of a continuous granulation process using a  
<sup>15</sup> twin-screw extruder, Int. J. Pharm. 356 (1-2) (2008) 224–230. doi:10.1016/j.ijpharm.2008.01.012.
- <sup>16</sup> [3] C. Vervaet, J. P. Remon, Continuous granulation in the pharmaceutical industry, Chem. Eng. Sci.  
<sup>17</sup> 60 (14) (2005) 3949–3957. doi:10.1016/j.ces.2005.02.028.
- <sup>18</sup> [4] J. Vercruyse, U. Delaet, I. V. Assche, P. Cappuyns, F. Arata, G. Caporicci, T. D. Beer, J. Remon,  
<sup>19</sup> C. Vervaet, Stability and repeatability of a continuous twin screw granulation and drying system, Eur.  
<sup>20</sup> J. Pharm. Biopharm. 85 (3, Part B) (2013) 1031 – 1038. doi:10.1016/j.ejpb.2013.05.002.
- <sup>21</sup> [5] J. Vercruyse, A. Burggraeve, M. Fonteyne, P. Cappuyns, U. Delaet, I. V. Assche, T. D. Beer, J. Remon,  
<sup>22</sup> C. Vervaet, Impact of screw configuration on the particle size distribution of granules produced by twin  
<sup>23</sup> screw granulation, Int. J. Pharm. 479 (1) (2015) 171 – 180. doi:10.1016/j.ijpharm.2014.12.071.
- <sup>24</sup> [6] R. M. Dhenge, J. J. Cartwright, M. J. Hounslow, A. D. Salman, Twin screw wet granulation: Effects of  
<sup>25</sup> properties of granulation liquid, Powder Technol. 229 (2012) 126–136. doi:10.1016/j.powtec.2012.06.019.

- 1 [7] R. M. Dhenge, K. Washino, J. J. Cartwright, M. J. Hounslow, A. D. Salman, Twin screw granulation  
2 using conveying screws: Effects of viscosity of granulation liquids and flow of powders, Powder Technol.  
3 238 (2013) 77–90. doi:10.1016/j.powtec.2012.05.045.
- 4 [8] M. Fonteyne, H. Wickström, E. Peeters, J. Vercruyse, H. Ehlers, B.-H. Peters, J. P. Remon, C. Vervaet,  
5 J. Ketolainen, N. Sandler, J. Rantanen, K. Naelapää, T. De Beer, Influence of raw material proper-  
6 ties upon critical quality attributes of continuously produced granules and tablets, Eur. J. Pharm.  
7 Biopharm. 87 (2) (2014) 252 – 263. doi:10.1016/j.ejpb.2014.02.011.
- 8 [9] A. S. El Hagras, J. R. Hennenkamp, M. D. Burke, J. J. Cartwright, J. D. Litster, Twin screw wet  
9 granulation: Influence of formulation parameters on granule properties and growth behavior, Powder  
10 Technol. 238 (2013) 108–115. doi:10.1016/j.powtec.2012.04.035.
- 11 [10] D. Djuric, Continuous granulation with a twin-screw extruder, Cuvillier Verlag, 2008.
- 12 [11] A. S. El Hagras, J. D. Litster, Granulation rate processes in the kneading elements of a twin screw  
13 granulator, AIChE J. 59 (11) (2013) 4100–4115. doi:10.1002/aic.14180.
- 14 [12] R. Sayin, A. E. Hagras, J. Litster, Distributive mixing elements: Towards improved granule attributes  
15 from a twin screw granulation process, Chemical Engineering Science 125 (0) (2015) 165 – 175, phar-  
16 maceutical Particles and Processing. doi:10.1016/j.ces.2014.06.040.
- 17 [13] M. R. Thompson, J. Sun, Wet granulation in a twin-screw extruder: Implications of screw design, J.  
18 Pharm. Sci. 99 (4) (2010) 2090–2103. doi:10.1002/jps.21973.
- 19 [14] R. M. Dhenge, J. J. Cartwright, D. G. Doughty, M. J. Hounslow, A. D. Salman, Twin screw  
20 wet granulation: Effect of powder feed rate, Adv. Powder Technol. 22 (2) (2011) 162 – 166.  
21 doi:10.1016/j.apt.2010.09.004.
- 22 [15] J. Litster, B. Ennis, The science and engineering of granulation processes, Vol. 15, Springer, 2004.
- 23 [16] D. Kayrak-Talay, S. Dale, C. Wassgren, J. Litster, Quality by design for wet granulation in  
24 pharmaceutical processing: Assessing models for a priori design and scaling, Powder Tech-  
25 nol. doi:10.1016/j.powtec.2012.07.013.
- 26 [17] K. P. Hapgood, J. D. Litster, R. Smith, Nucleation regime map for liquid bound granules, AIChE J.  
27 49 (2) (2003) 350–361. doi:10.1002/aic.690490207.
- 28 [18] S. M. Iveson, P. A. Wauters, S. Forrest, J. D. Litster, G. M. Meesters, B. Scarlett, Growth regime map  
29 for liquid-bound granules: further development and experimental validation, Powder Technol. 117 (1)  
30 (2001) 83 – 97, granulation and Coating of Fine Powders. doi:10.1016/S0032-5910(01)00317-5.
- 31 [19] S. Rough, D. Wilson, D. York, A regime map for stages in high shear mixer agglomeration using ultra-  
32 high viscosity binders, Adv. Powder Technol. 16 (4) (2005) 373 – 386. doi:10.1163/1568552054194186.
- 33 [20] W.-D. Tu, A. Ingram, J. Seville, S.-S. Hsiau, Exploring the regime map for high-shear mixer granulation,  
34 Chem. Eng. J. 145 (3) (2009) 505 – 513. doi:10.1016/j.cej.2008.09.033.

- 1 [21] W.-D. Tu, A. Ingram, J. Seville, Regime map development for continuous twin screw granulation,  
2 Chem. Eng. Sci. 87 (2013) 315–326. doi:10.1016/j.ces.2012.08.015.
- 3 [22] L. Eriksson, Design of Experiments: Principles and Applications, Umetrics, 2008.
- 4 [23] C. Martin, Twin screw extrusion for pharmaceutical processes, in: M. A. Repka, N. Langley, J. DiNunzio  
5 (Eds.), Melt Extrusion, Vol. 9 of AAPS Advances in the Pharmaceutical Sciences Series, Springer New  
6 York, 2013, pp. 47–79.
- 7 [24] PIV Drives GmbH, Gearboxes and drive packages for extrusion, compounding and injection moulding  
8 machines (mar 2014).
- 9 URL <http://www.brevini.com/wp-content/uploads/2014/03/B030-PIV-Drives-Plastic-and-Rubber-EN.pdf>
- 10 [25] B. B. Weiner, What is a continuous particle size distribution, Brookhaven Instruments Corporation  
11 White Paper, Holtsville.
- 12 [26] R. Sibson, A brief description of natural neighbour interpolation, Interpreting multivariate data 21.
- 13 [27] A. Kumar, J. Vercruyse, G. Bellandi, K. V. Gernaey, C. Vervaet, J. P. Remon, T. D. Beer, I. Nopens,  
14 Experimental investigation of granule size and shape dynamics in twin-screw granulation, Int. J. Pharm.  
15 475 (1-2) (2014) 485 – 495. doi:10.1016/j.ijpharm.2014.09.020.
- 16 [28] K. T. Lee, A. Ingram, N. A. Rowson, Twin screw wet granulation: the study of a continuous twin screw  
17 granulator using Positron Emission Particle Tracking (PEPT) technique., Eur. J. Pharm. Biopharm.  
18 81 (3) (2012) 666–73. doi:10.1016/j.ejpb.2012.04.011.
- 19 [29] K. P. Hapgood, S. M. Iveson, J. D. Litster, L. X. Liu, A. Salman, M. Hounslow, J. Seville, Granulation  
20 rate processes, Granulation 11 (2007) 897–977.
- 21 [30] M. Zlokarnik, Dimensional analysis and scale-up in theory and industrial application, Informa Health-  
care, 2011, Ch. 1, pp. 1–57. doi:10.3109/9781616310028.001.
- 22 [31] J. Bouffard, F. Bertrand, J. Chaouki, A multiscale model for the simulation of granulation in rotor-  
23 based equipment, Chem. Eng. Sci. 81 (2012) 106–117. doi:10.1016/j.ces.2012.06.025.
- 24 [32] M. Hussain, J. Kumar, M. Peglow, E. Tsotsas, On two-compartment population balance mod-  
eling of spray fluidized bed agglomeration, Comp. Chem. Eng. 61 (0) (2014) 185 – 202.  
doi:10.1016/j.compchemeng.2013.11.003.
- 25 [33] D. Barrasso, R. Ramachandran, Multi-scale modeling of granulation processes: Bi-directional coupling  
26 of PBM with DEM via collision frequencies, Chemical Engineering Research and Design 93 (0) (2015)  
27 304 – 317. doi:10.1016/j.cherd.2014.04.016.
- 28 [34] A. Kumar, K. V. Gernaey, T. De Beer, I. Nopens, Model-based characterisation of twin-screw gran-  
29 ulation system for continuous solid dosage manufacturing, Comput. Aided Chem. Eng. 37 (0) (2015)  
30 2165–2170.

## <sup>1</sup> List of Figures

2	1	Granule growth regime map for twin screw granulation based on the deformation values ( $\beta$ ) and pore saturation as a function of L/S and viscosity of the granulation liquid, i.e. L/S $\times$ viscosity proposed by Dhenge et al. [6]. . . . .	21
5	2	Twin-screw granulator screws with two kneading blocks. . . . .	22
6	3	Response contour of the change in the torque level at different screw speeds (500, 700, 900 rpm), material throughputs (10-25 kg/h), number of kneading discs (1 $\times$ 6, 2 $\times$ 6) and stagger angle (60°) during twin-screw granulation. . . . .	23
9	4	GSD at different screw speeds (500, 700, 900 rpm), material throughputs (10-25 kg/h), number of kneading discs (1 $\times$ 6, 2 $\times$ 6), stagger angle (60°) and liquid-to-solid ratio (8-10 %) [MFR: material throughput (kg/h), NK: number of kneading discs (-), RPM: screw speed (rpm), LSR: liquid-to-solid ratio]. . . . .	24
13	5	Response contour of the change in fines fraction (<150 $\mu$ m) in the granules produced at different screw speeds (500, 700, 900 rpm), material throughputs (10-25 kg/h), number of kneading discs (1 $\times$ 6, 2 $\times$ 6) and stagger angle (60°). . . . .	25
16	6	Response contour of the change in yield fraction (150 - 1400 $\mu$ m) in the granules produced at different screw speeds (500, 700, 900 rpm), material throughputs (10-25 kg/h), number of kneading discs (1 $\times$ 6, 2 $\times$ 6) and stagger angle (60°). . . . .	26
20	7	Response contour of the change in oversized fraction (>1400 $\mu$ m) in the granules produced at different screw speeds (500, 700, 900 rpm), material throughputs (10-25 kg/h), number of kneading discs (1 $\times$ 6, 2 $\times$ 6) and stagger angle (60°). . . . .	27
24	8	Response contour of the change in specific mechanical energy input level at different screw speeds (500, 700, 900 rpm), material throughputs (10-25 kg/h), number of kneading discs (1 $\times$ 6, 2 $\times$ 6) and stagger angle (60°) during twin-screw granulation. . . . .	28
28	9	Process map indicating the change in percentile values ( $D_{25}$ , $D_{50}$ , $D_{75}$ ) of the granule size distribution with change in L/S ratio and specific mechanical energy input. . . . .	29
31	10	Change in the percentile ratio ( $D_{75}/D_{25}$ ) of the granule size distribution with change in L/S ratio and specific mechanical energy input. . . . .	30
33	11	Steps required to develop a generalised granulation regime map for twin-screw granulation . . . . .	31

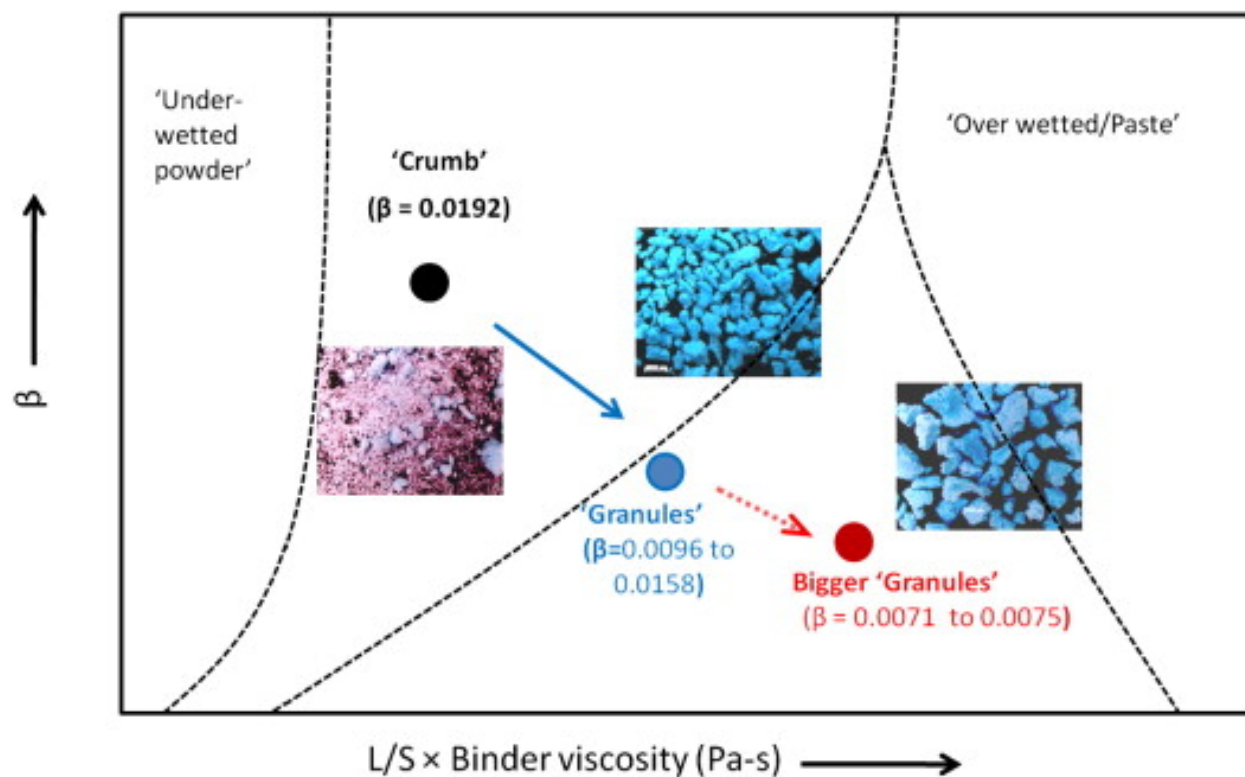


Figure 1: Granule growth regime map for twin screw granulation based on the deformation values ( $\beta$ ) and pore saturation as a function of  $L/S$  and viscosity of the granulation liquid, i.e.  $L/S \times$  viscosity proposed by Dhenge et al. [6].

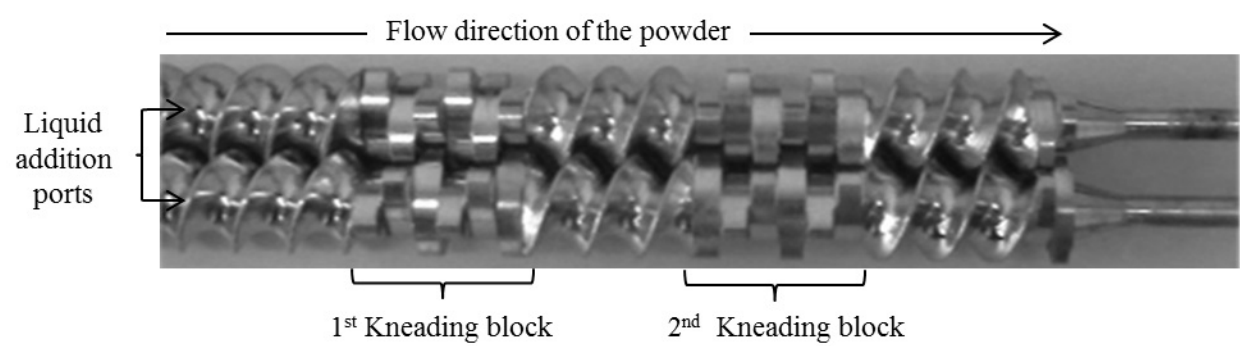


Figure 2: Twin-screw granulator screws with two kneading blocks.

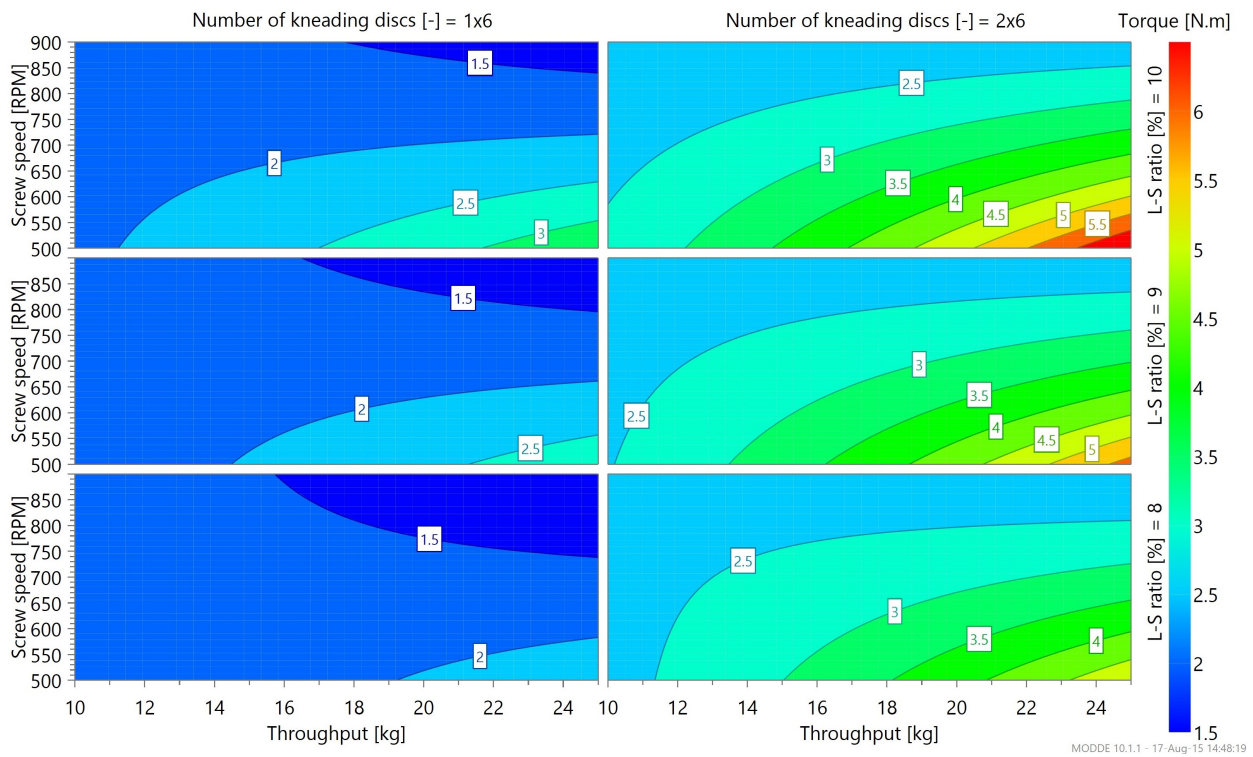


Figure 3: Response contour of the change in the torque level at different screw speeds (500, 700, 900 rpm), material throughputs (10-25 kg/h), number of kneading discs ( $1 \times 6$ ,  $2 \times 6$ ) and stagger angle ( $60^\circ$ ) during twin-screw granulation.

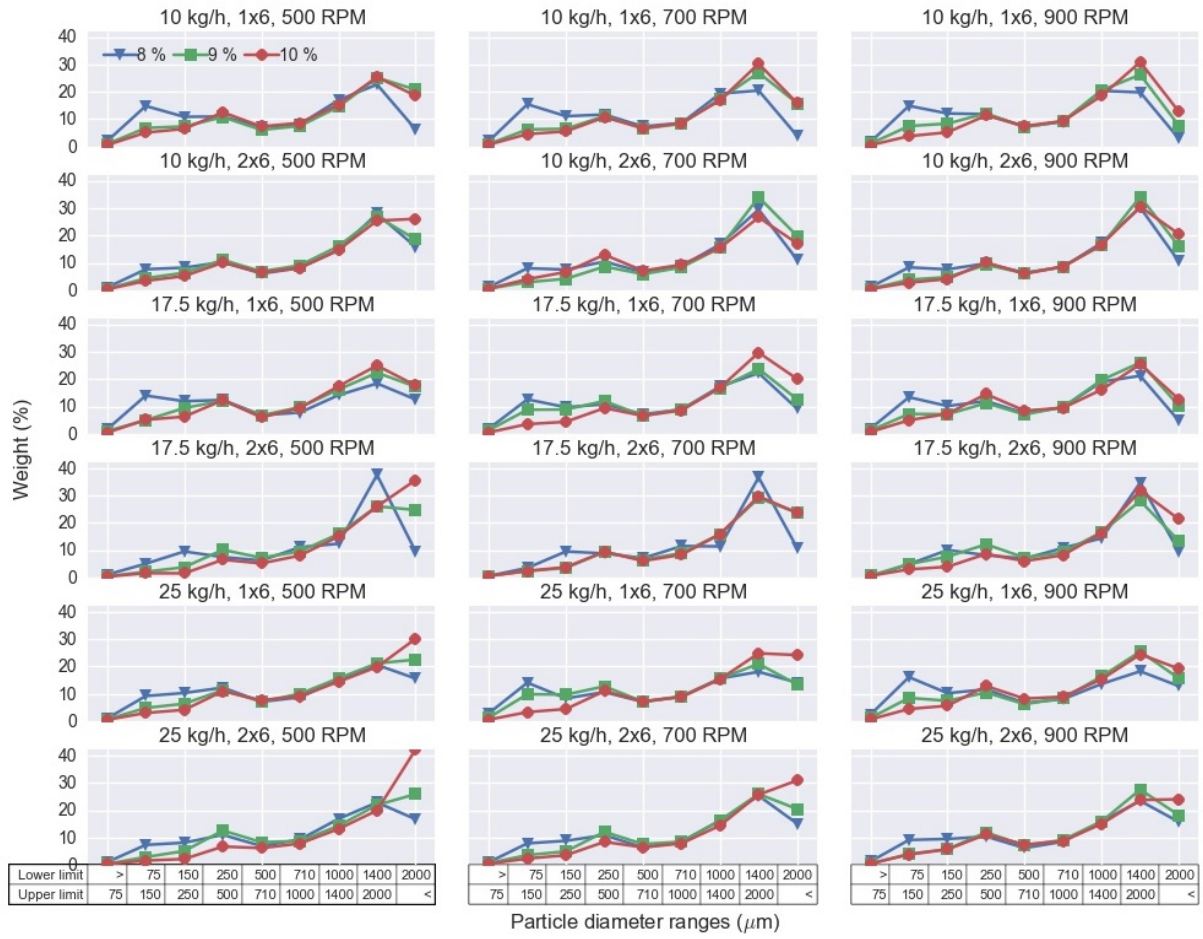


Figure 4: GSD at different screw speeds (500, 700, 900 rpm), material throughputs (10-25 kg/h), number of kneading discs (1×6, 2×6), stagger angle (60°) and liquid-to-solid ratio (8-10 %) [MFR: material throughput (kg/h), NK: number of kneading discs (-), RPM: screw speed (rpm), LSR: liquid-to-solid ratio].

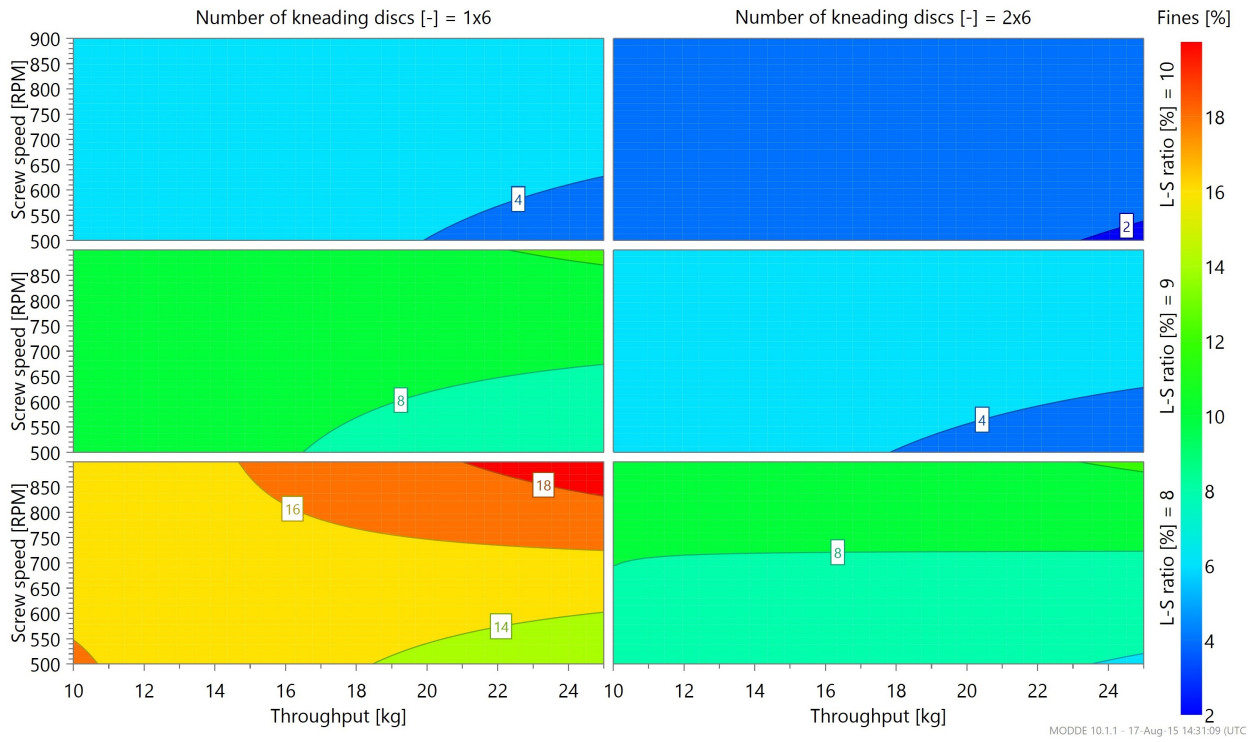


Figure 5: Response contour of the change in fines fraction ( $<150 \mu\text{m}$ ) in the granules produced at different screw speeds (500, 700, 900 rpm), material throughputs (10-25 kg/h), number of kneading discs (1 $\times$ 6, 2 $\times$ 6) and stagger angle ( $60^\circ$ ).

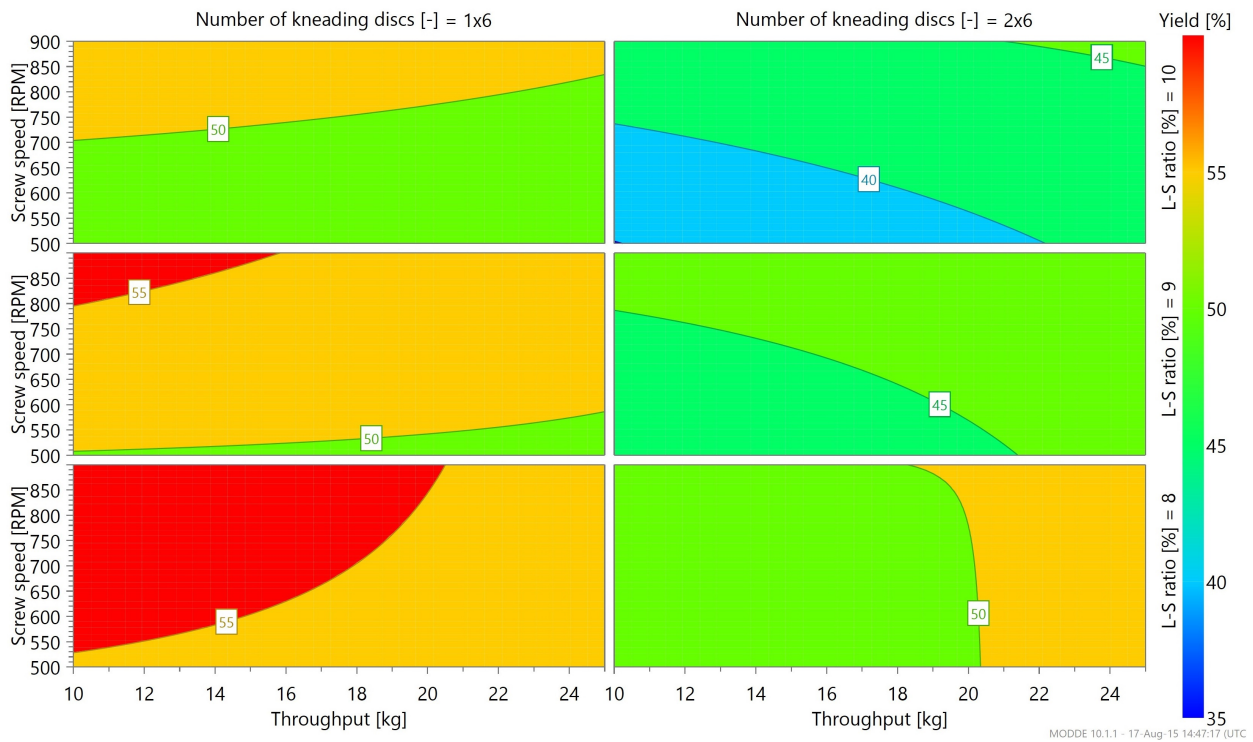


Figure 6: Response contour of the change in yield fraction (150 - 1400  $\mu\text{m}$ ) in the granules produced at different screw speeds (500, 700, 900 rpm), material throughputs (10-25 kg/h), number of kneading discs (1 $\times$ 6, 2 $\times$ 6) and stagger angle ( $60^\circ$ ).

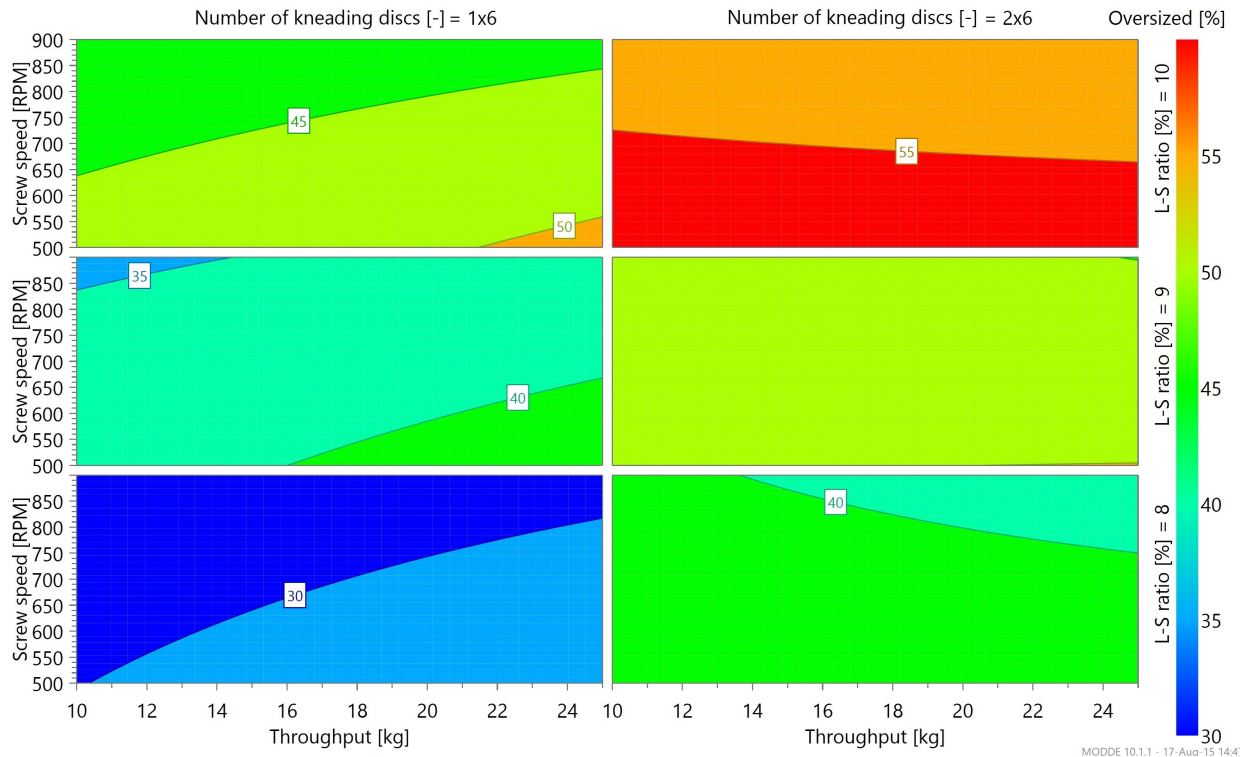


Figure 7: Response contour of the change in oversized fraction ( $>1400 \mu\text{m}$ ) in the granules produced at different screw speeds (500, 700, 900 rpm), material throughputs (10-25 kg/h), number of kneading discs (1x6, 2x6) and stagger angle ( $60^\circ$ ).

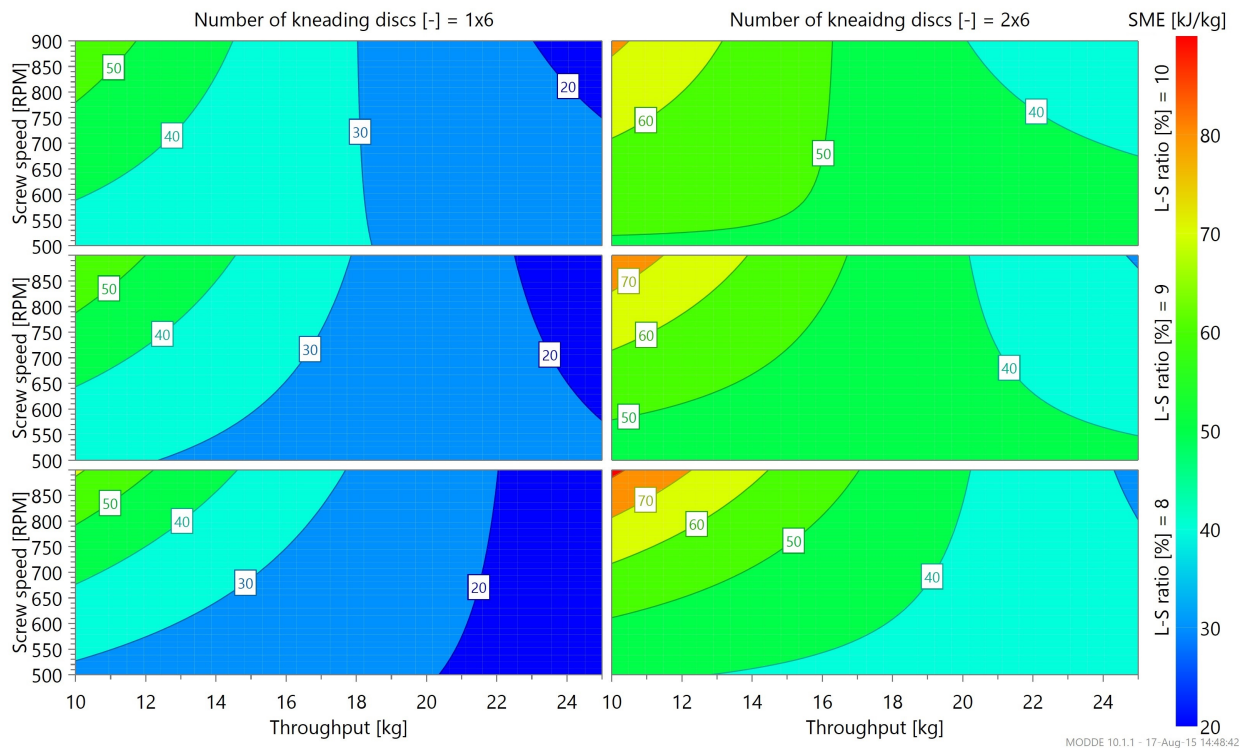


Figure 8: Response contour of the change in specific mechanical energy input level at different screw speeds (500, 700, 900 rpm), material throughputs (10-25 kg/h), number of kneading discs ( $1 \times 6$ ,  $2 \times 6$ ) and stagger angle ( $60^\circ$ ) during twin-screw granulation.

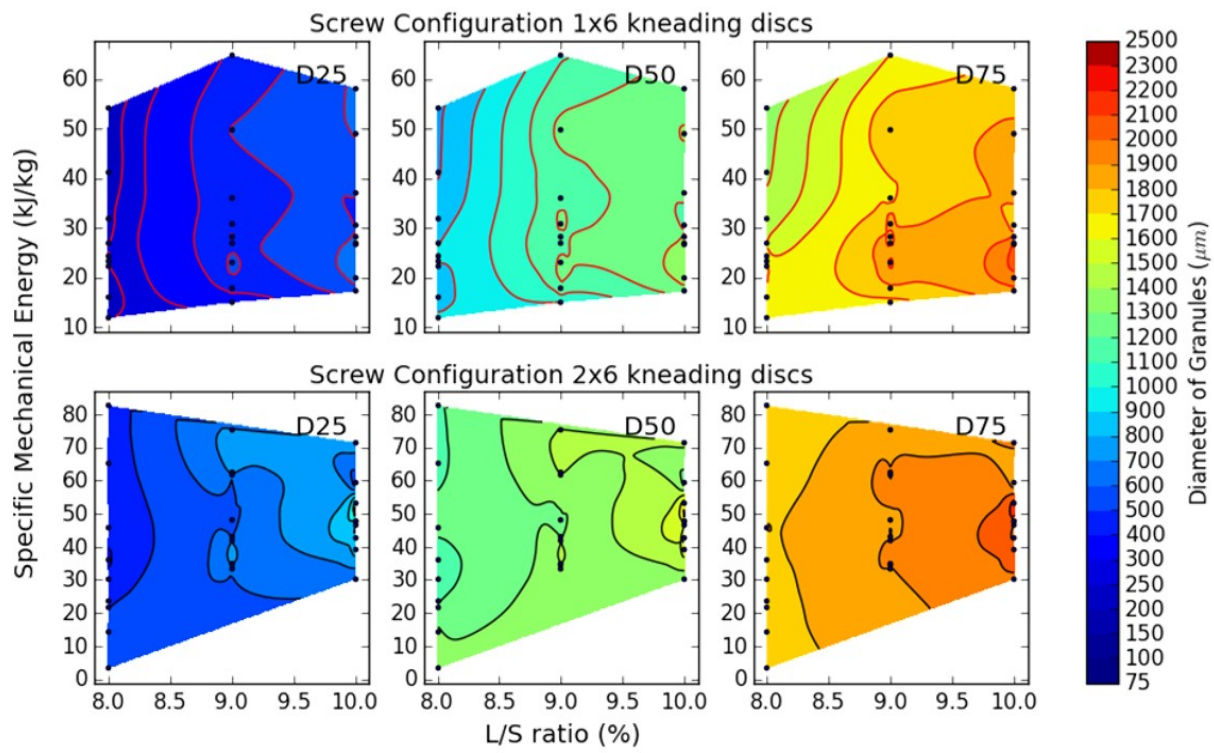


Figure 9: Process map indicating the change in percentile values (D<sub>25</sub>, D<sub>50</sub>, D<sub>75</sub>) of the granule size distribution with change in L/S ratio and specific mechanical energy input.

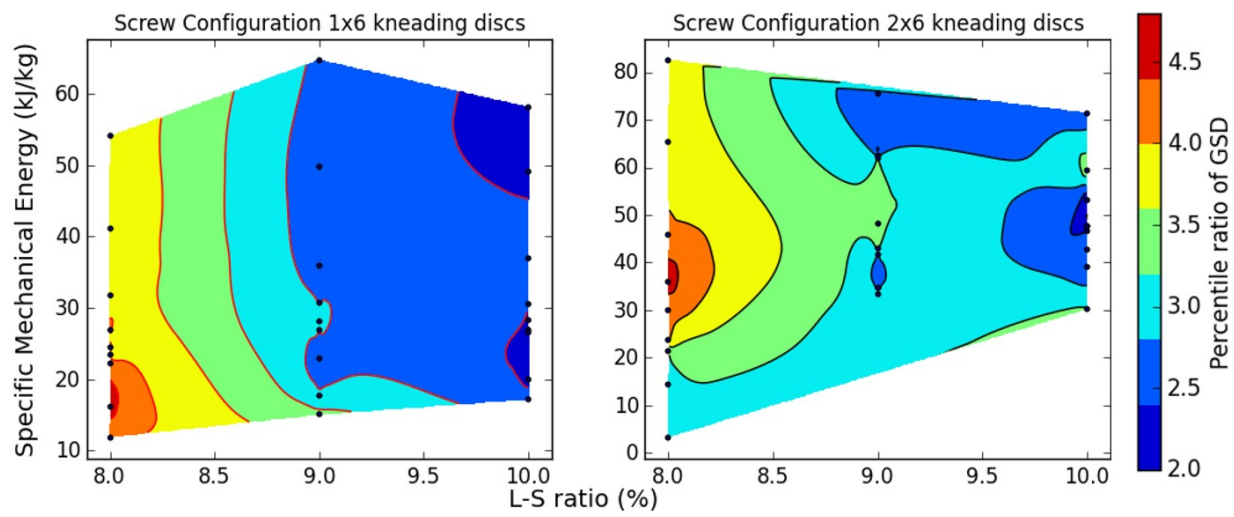


Figure 10: Change in the percentile ratio ( $D_{75}/D_{25}$ ) of the granule size distribution with change in L/S ratio and specific mechanical energy input.

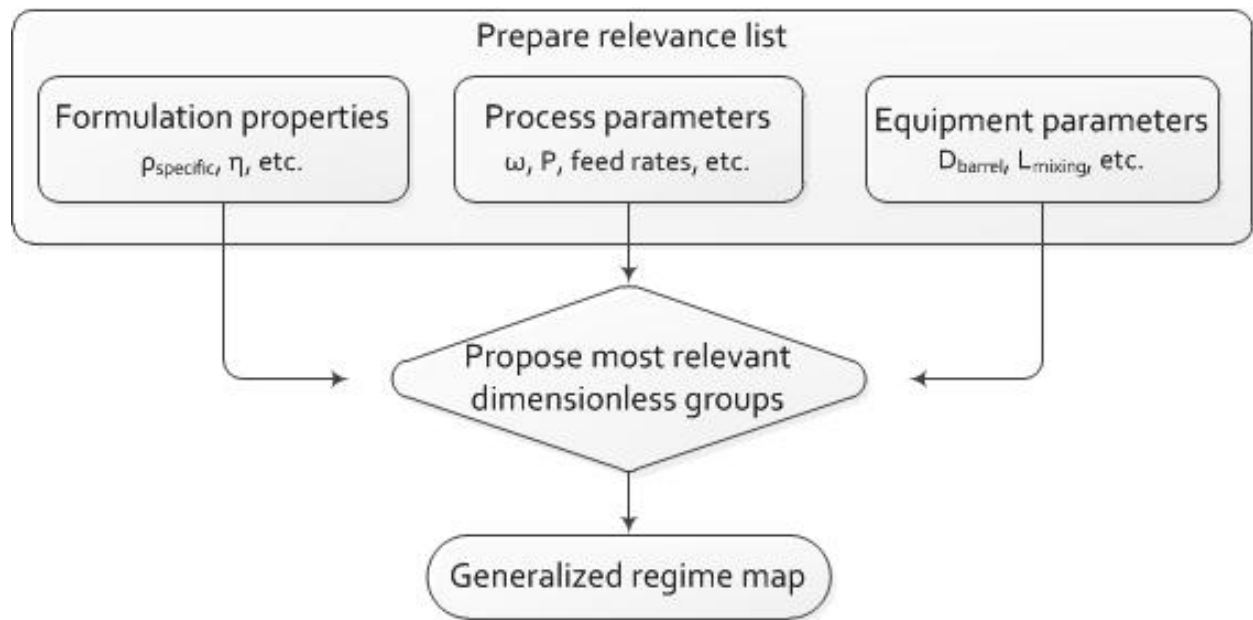


Figure 11: Steps required to develop a generalised granulation regime map for twin-screw granulation